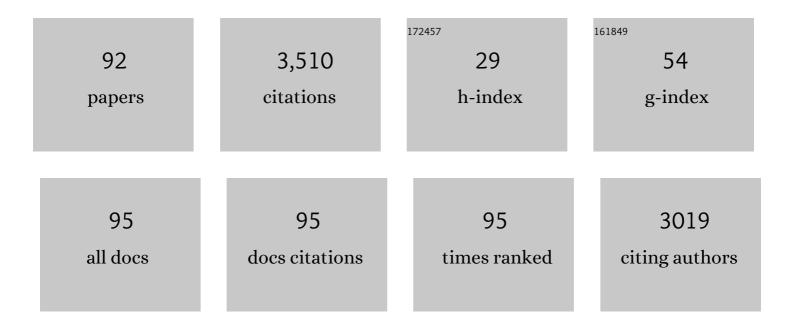
## Jason Olfert

List of Publications by Year in descending order

Source: https://exaly.com/author-pdf/7028247/publications.pdf Version: 2024-02-01



LASON OLEEDT

#	Article	lF	CITATIONS
1	Radiative Absorption Enhancements Due to the Mixing State of Atmospheric Black Carbon. Science, 2012, 337, 1078-1081.	12.6	618
2	Soot Particle Studies—Instrument Inter-Comparison—Project Overview. Aerosol Science and Technology, 2010, 44, 592-611.	3.1	228
3	The effective density and fractal dimension of particles emitted from a light-duty diesel vehicle with a diesel oxidation catalyst. Journal of Aerosol Science, 2007, 38, 69-82.	3.8	176
4	Effective density of Aquadag and fullerene soot black carbon reference materials used for SP2 calibration. Atmospheric Measurement Techniques, 2011, 4, 2851-2858.	3.1	157
5	The Detection Efficiency of the Single Particle Soot Photometer. Aerosol Science and Technology, 2010, 44, 612-628.	3.1	151
6	New method for particle mass classification—the Couette centrifugal particle mass analyzer. Journal of Aerosol Science, 2005, 36, 1338-1352.	3.8	139
7	Diesel soot mass calculation in real-time with a differential mobility spectrometer. Journal of Aerosol Science, 2007, 38, 52-68.	3.8	132
8	Mass, Mobility, Volatility, and Morphology of Soot Particles Generated by a McKenna and Inverted Burner. Aerosol Science and Technology, 2013, 47, 395-405.	3.1	70
9	Determination of particle mass, effective density, mass–mobility exponent, and dynamic shape factor using an aerodynamic aerosol classifier and a differential mobility analyzer in tandem. Journal of Aerosol Science, 2014, 75, 35-42.	3.8	67
10	Particle effective density and mass during steady-state operation of GDI, PFI, and diesel passenger cars. Journal of Aerosol Science, 2015, 83, 39-54.	3.8	65
11	Universal relations between soot effective density and primary particle size for common combustion sources. Aerosol Science and Technology, 2019, 53, 485-492.	3.1	62
12	Soot Aggregate Restructuring Due to Coatings of Secondary Organic Aerosol Derived from Aromatic Precursors. Environmental Science & Technology, 2014, 48, 14309-14316.	10.0	59
13	Coating Mass Dependence of Soot Aggregate Restructuring due to Coatings of Oleic Acid and Dioctyl Sebacate. Aerosol Science and Technology, 2013, 47, 192-200.	3.1	58
14	Comprehensive characterization of mainstream marijuana and tobacco smoke. Scientific Reports, 2020, 10, 7160.	3.3	51
15	An Instrument for the Classification of Aerosols by Particle Relaxation Time: Theoretical Models of the Aerodynamic Aerosol Classifier. Aerosol Science and Technology, 2013, 47, 916-926.	3.1	49
16	Characterization of Particulate Matter Morphology and Volatility from a Compression-Ignition Natural-Gas Direct-Injection Engine. Aerosol Science and Technology, 2015, 49, 589-598.	3.1	49
17	Measuring aerosol size distributions with the fast integrated mobility spectrometer. Journal of Aerosol Science, 2008, 39, 940-956.	3.8	45
18	Effective Density and Volatility of Particles Emitted from Gasoline Direct Injection Vehicles and Implications for Particle Mass Measurement. Aerosol Science and Technology, 2015, 49, 1051-1062.	3.1	45

#	Article	lF	CITATIONS
19	Variation of the optical properties of soot as a function of particle mass. Carbon, 2017, 124, 201-211.	10.3	42
20	Steady-state measurement of the effective particle density of cigarette smoke. Journal of Aerosol Science, 2014, 75, 9-16.	3.8	41
21	The experimental transfer function of the Couette centrifugal particle mass analyzer. Journal of Aerosol Science, 2006, 37, 1840-1852.	3.8	40
22	Measuring aerosol size distributions with the aerodynamic aerosol classifier. Aerosol Science and Technology, 2018, 52, 655-665.	3.1	39
23	Size, effective density, morphology, and nano-structure of soot particles generated from buoyant turbulent diffusion flames. Journal of Aerosol Science, 2019, 132, 22-31.	3.8	38
24	Response to Comment on "Radiative Absorption Enhancements Due to the Mixing State of Atmospheric Black Carbon". Science, 2013, 339, 393-393.	12.6	35
25	Particle Emission Characteristics of a Gas Turbine with a Double Annular Combustor. Aerosol Science and Technology, 2015, 49, 842-855.	3.1	35
26	Measurement and modeling of the multiwavelength optical properties of uncoated flame-generated soot. Atmospheric Chemistry and Physics, 2018, 18, 12141-12159.	4.9	35
27	Overview of the Cumulus Humilis Aerosol Processing Study. Bulletin of the American Meteorological Society, 2009, 90, 1653-1668.	3.3	33
28	Deposition of Inhaled Ultrafine Aerosols in Replicas of Nasal Airways of Infants. Aerosol Science and Technology, 2010, 44, 741-752.	3.1	31
29	Effective Density and Mass-Mobility Exponent of Aircraft Turbine Particulate Matter. Journal of Propulsion and Power, 2015, 31, 573-582.	2.2	31
30	Mass–Mobility Measurements Using a Centrifugal Particle Mass Analyzer and Differential Mobility Spectrometer. Aerosol Science and Technology, 2013, 47, 1215-1225.	3.1	29
31	The CPMA-Electrometer System—A Suspended Particle Mass Concentration Standard. Aerosol Science and Technology, 2013, 47, i-iv.	3.1	29
32	A novel miniature inverted-flame burner for the generation of soot nanoparticles. Aerosol Science and Technology, 2019, 53, 184-195.	3.1	29
33	Viral load of SARS-CoV-2 in droplets and bioaerosols directly captured during breathing, speaking and coughing. Scientific Reports, 2022, 12, 3484.	3.3	28
34	Generation of a Monodisperse Size-Classified Aerosol Independent of Particle Charge. Aerosol Science and Technology, 2014, 48, i-iv.	3.1	27
35	Morphology and size of soot from gas flares as a function of fuel and water addition. Fuel, 2020, 279, 118478.	6.4	27
36	Methodology for quantifying the volatile mixing state of an aerosol. Aerosol Science and Technology, 2016, 50, 759-772.	3.1	26

#	Article	IF	CITATIONS
37	Effective density and volatility of particles sampled from a helicopter gas turbine engine. Aerosol Science and Technology, 2017, 51, 704-714.	3.1	26
38	Morphology and volatility of particulate matter emitted from a gasoline direct injection engine fuelled on gasoline and ethanol blends. Journal of Aerosol Science, 2017, 105, 166-178.	3.8	26
39	Principal component analysis of summertime ground site measurements in the Athabasca oil sands with a focus on analytically unresolved intermediate-volatility organic compounds. Atmospheric Chemistry and Physics, 2018, 18, 17819-17841.	4.9	26
40	Characterising mass-resolved mixing state of black carbon in Beijing using a morphology-independent measurement method. Atmospheric Chemistry and Physics, 2020, 20, 3645-3661.	4.9	26
41	Effect of electrostatic charge on oral-extrathoracic deposition for uniformly charged monodisperse aerosols. Journal of Aerosol Science, 2014, 68, 38-45.	3.8	25
42	Characterization of black carbon particles generated by a propane-fueled miniature inverted soot generator. Journal of Aerosol Science, 2019, 135, 46-57.	3.8	25
43	Improved sizing of soot primary particles using mass-mobility measurements. Aerosol Science and Technology, 2016, 50, 101-109.	3.1	22
44	Relative Humidity Dependence of Soot Aggregate Restructuring Induced by Secondary Organic Aerosol: Effects of Water on Coating Viscosity and Surface Tension. Environmental Science and Technology Letters, 2017, 4, 386-390.	8.7	22
45	Calibration of optical particle counters with an aerodynamic aerosol classifier. Journal of Aerosol Science, 2019, 138, 105452.	3.8	21
46	Inversion methods to determine two-dimensional aerosol mass-mobility distributions: A critical comparison of established methods. Journal of Aerosol Science, 2020, 140, 105484.	3.8	21
47	Effect of Induced Charge on Deposition of Uniformly Charged Particles in a Pediatric Oral-Extrathoracic Airway. Aerosol Science and Technology, 2014, 48, 508-514.	3.1	20
48	Measuring the bipolar charge distribution of nanoparticles: Review of methodologies and development using the Aerodynamic Aerosol Classifier. Journal of Aerosol Science, 2020, 143, 105526.	3.8	20
49	Effect of Electrostatic Charge on Deposition of Uniformly Charged Monodisperse Particles in the Nasal Extrathoracic Airways of an Infant. Journal of Aerosol Medicine and Pulmonary Drug Delivery, 2015, 28, 30-34.	1.4	18
50	Enhanced Evaporation of Microscale Droplets With an Infrared Laser. Journal of Heat Transfer, 2017, 139, .	2.1	17
51	Relationship between Coating-Induced Soot Aggregate Restructuring and Primary Particle Number. Environmental Science & Technology, 2017, 51, 8376-8383.	10.0	17
52	Size, volatility, and effective density of particulate emissions from a homogeneous charge compression ignition engine using compressed natural gas. Journal of Aerosol Science, 2014, 75, 1-8.	3.8	15
53	Demonstration of the CPMA-Electrometer System for Calibrating Black Carbon Particulate Mass Instruments. Aerosol Science and Technology, 2015, 49, 152-158.	3.1	15
54	The effect of sodium chloride on the nanoparticles observed in a laminar methane diffusion flame. Combustion and Flame, 2018, 188, 273-283.	5.2	15

#	Article	IF	CITATIONS
55	Properties of carbon black produced by the thermal decomposition of methane in the products of premixed flames. Journal of Aerosol Science, 2019, 131, 13-27.	3.8	15
56	Dynamic Characteristics of a Fast-Response Aerosol Size Spectrometer. Aerosol Science and Technology, 2009, 43, 97-111.	3.1	14
57	Effect of Thermodenuding on the Structure of Nascent Flame Soot Aggregates. Atmosphere, 2017, 8, 166.	2.3	14
58	Transient measurement of the effective particle density of cigarette smoke. Journal of Aerosol Science, 2015, 87, 63-74.	3.8	13
59	A novel inversion method to determine the mass distribution of non-refractory coatings on refractory black carbon using a centrifugal particle mass analyzer and single particle soot photometer. Aerosol Science and Technology, 2018, 52, 567-578.	3.1	13
60	Quantifying the carbon conversion efficiency and emission indices of a lab-scale natural gas flare with internal coflows of air or steam. Experimental Thermal and Fluid Science, 2019, 103, 133-142.	2.7	13
61	Closure between particulate matter concentrations measured ex situ by thermal–optical analysis and in situ by the CPMA–electrometer reference mass system. Aerosol Science and Technology, 2020, 54, 1293-1309.	3.1	13
62	AN ATOMIZER TO GENERATE MONODISPERSE DROPLETS FROM HIGH VAPOR PRESSURE LIQUIDS. Atomization and Sprays, 2016, 26, 121-134.	0.8	13
63	Probe sampling to map and characterize nanoparticles along the axis of a laminar methane jet diffusion flame. Proceedings of the Combustion Institute, 2017, 36, 881-888.	3.9	12
64	New approaches to calculate the transfer function of particle mass analyzers. Aerosol Science and Technology, 2020, 54, 111-127.	3.1	12
65	Determining the cutoff diameter and counting efficiency of optical particle counters with an aerodynamic aerosol classifier and an inkjet aerosol generator. Aerosol Science and Technology, 2020, 54, 1335-1344.	3.1	12
66	A Numerical Calculation of the Transfer Function of the Fluted Centrifugal Particle Mass Analyzer. Aerosol Science and Technology, 2005, 39, 1002-1009.	3.1	11
67	Performance of Pressurized Meteredâ€Dose Inhalers at Extreme Temperature Conditions. Journal of Pharmaceutical Sciences, 2014, 103, 3553-3559.	3.3	11
68	Comparison of Particle Number Emissions from In-Flight Aircraft Fueled with Jet A1, JP-5 and an Alcohol-to-Jet Fuel Blend. Energy & Fuels, 2020, 34, 7218-7222.	5.1	11
69	Aerosol penetration in microchannels. Journal of Aerosol Science, 2011, 42, 321-328.	3.8	10
70	Hygroscopic effects on the mobility and mass of cigarette smoke particles. Journal of Aerosol Science, 2015, 86, 69-78.	3.8	10
71	Inversion methods to determine two-dimensional aerosol mass-mobility distributions II: Existing and novel Bayesian methods. Journal of Aerosol Science, 2020, 146, 105565.	3.8	10
72	Comparison of emissions from steam- and water-assisted lab-scale flames. Fuel, 2021, 302, 121107.	6.4	10

#	Article	IF	CITATIONS
73	Effect of sodium chloride on the evolution of size, mixing state, and light absorption of soot particles from a smoking laminar diffusion flame. Combustion and Flame, 2020, 218, 168-178.	5.2	8
74	Generating an aerosol of homogeneous, non-spherical particles and measuring their bipolar charge distribution. Journal of Aerosol Science, 2021, 153, 105705.	3.8	8
75	Using two-dimensional distributions to inform the mixing state of soot and salt particles produced in gas flares. Journal of Aerosol Science, 2021, 158, 105826.	3.8	8
76	Real-time driving cycle measurements of ultrafine particle emissions from two wheelers and comparison with passenger cars. International Journal of Automotive Technology, 2014, 15, 1053-1061.	1.4	7
77	Particulate emissions from turbulent diffusion flames with entrained droplets: A laboratory simulation of gas flaring emissions. Journal of Aerosol Science, 2021, 157, 105807.	3.8	7
78	Effect of Engine-Out Soot Emissions and the Frequency of Regeneration on Gasoline Particulate Filter Efficiency. , 0, , .		7
79	Determination of particle temperatures in a silica-generating counterflow flame via flame emission measurements. International Journal of Heat and Mass Transfer, 2010, 53, 564-567.	4.8	6
80	Effect of fuel choice on nanoparticle emission factors in LPG-gasoline bi-fuel vehicles. International Journal of Automotive Technology, 2013, 14, 1-11.	1.4	6
81	The Effect of Altitude on Inhaler Performance. Journal of Pharmaceutical Sciences, 2014, 103, 2116-2124.	3.3	6
82	Repeatability and intermediate precision of a mass concentration calibration system. Aerosol Science and Technology, 2019, 53, 701-711.	3.1	6
83	Modification of the TSI 3081 differential mobility analyzer to include three monodisperse outlets: Comparison between experimental and theoretical performance. Aerosol Science and Technology, 2016, 50, 1342-1351.	3.1	5
84	An improved inversion method for determining two-dimensional mass distributions of non-refractory materials on refractory black carbon. Aerosol Science and Technology, 2021, 55, 104-118.	3.1	5
85	Acoustic method for measuring the sound speed of gases over small path lengths. Review of Scientific Instruments, 2007, 78, 054901.	1.3	4
86	Validation of MAX-DOAS retrievals of aerosol extinction, SO <sub>2</sub> , and NO <sub>2</sub> through comparison with lidar, sun photometer, active DOAS, and aircraft measurements in the Athabasca oil sands region. Atmospheric Measurement Techniques, 2020, 13, 1129-1155.	3.1	4
87	Accelerated measurements of aerosol size distributions by continuously scanning the aerodynamic aerosol classifier. Aerosol Science and Technology, 2021, 55, 119-141.	3.1	3
88	Particle Size-Dependent Filtration Efficiency and Pressure Drop of Gasoline Particle Filters with Varying Washcoat Volumes. Emission Control Science and Technology, 2021, 7, 105-116.	1.5	2
89	Optimized instrument configurations for tandem particle mass analyzer and single particle-soot photometer experiments. Journal of Aerosol Science, 2022, 160, 105897.	3.8	2
90	An ultrasonic sound speed sensor for measuring exhaust gas recirculation levels. Proceedings of the Institution of Mechanical Engineers, Part D: Journal of Automobile Engineering, 2007, 221, 181-189.	1.9	1

#	Article	IF	CITATIONS
91	Development and testing of a universal aerosol conditioner. Aerosol Science and Technology, 2022, 56, 382-393.	3.1	1
92	A Fuel Quality Sensor for Fuel Cell Vehicles, Natural Gas Vehicles, and Variable Gaseous Fuel Vehicles. , 0, , .		0